Effect of Perfusion Pattern and Imaging Sequence on Gated Perfusion SPECT Evaluation of Myocardial Stunning

Alain Manrique, MD; Anne Hitzel, MD; David Brasse, PhD; and Pierre Véra, MD, PhD

Département de Médecine Nucléaire et Laboratoire Universitaire Quantification en Imagerie Fonctionelle, Centre Henri Becquerel, Rouen, France

The aim of this study was to determine the effect of perfusion defect and imaging sequence on the evaluation of myocardial stunning with gated perfusion SPECT. **Methods:** A dynamic mathematic cardiac torso phantom was used to create 100 gated SPECT simulations (50 stress–rest and 50 rest–stress sequences) with a wide range of perfusion defects. No segmental wall motion abnormalities were created. After generating projection images, 2 additional acquisitions were simulated by thresholding the projected data to 25% and 75% of the maximum. Finally, gated SPECT projections were grouped by 2s to generate 2 series of phantoms corresponding to stress–rest and rest–stress imaging sequences. For each sequence, the first dataset was the 25% thresholded gated SPECT. Both 75% thresholded and 100% signal intensity were used as a second dataset. Each simulated gated SPECT image differed from others in the extent of myocardial scar or ischemia, but all had the same end-diastolic volume (EDV) (125 mL), end-systolic volume (ESV) (48 mL), and ejection fraction (EF) (62%). Left ventricular perfusion and function were each assessed using validated software. **Results:** Mean stress EDV was decreased when compared with rest–simulated data (111 $\pm$ 4.7 and 112.4 $\pm$ 4.8 mL, respectively; $P \leq 0.05$), and mean stress ESV was increased when compared with rest–simulated data (44 $\pm$ 4.2 and 42.7 $\pm$ 4 mL, respectively; $P < 0.02$). The resulting mean stress EF was decreased in the same comparison (60.3% $\pm$ 3.1% and 62% $\pm$ 2.7%, respectively; $P = 0.0001$). After multivariate analysis, the difference between stress and rest EF was significantly influenced by myocardial infarction ($P = 0.0027$), severe extent of myocardial ischemia ($P = 0.0017$), and imaging sequence ($P < 0.0001$). A $\geq$5% decrease in EF on stress SPECT (i.e., myocardial stunning) was significantly associated with the stress–rest sequence ($\chi^2 = 26$; $P < 0.0001$). **Conclusion:** Perfusion defects and imaging sequence had significant effects on the evaluation of myocardial stunning using gated perfusion SPECT.

Key Words: cardiology; gated SPECT; imaging sequence; myocardial stunning; perfusion; technetium

J Nucl Med 2005; 46:176–183

Received Mar. 18, 2004; revision accepted Sep. 13, 2004.

For correspondence or reprints contact: Alain Manrique, MD, Département de Médecine Nucléaire et Laboratoire Universitaire Quant.IF. Centre Henri Becquerel, 1 rue d'Amiens, 76000 Rouen, France.

E-mail: alain.manrique@rouen.fnclcc.fr

Gated myocardial perfusion SPECT enables analysis of wall motion, wall thickening, and ejection fraction (EF) measurements with a combined assessment of myocardial perfusion and ventricular function by a single injection of a radiopharmaceutical agent. Although left ventricular (LV) volume determination requires endocardial edge detection based on myocardial perfusion, it has been demonstrated that gated SPECT provides reliable information on global LV function even in patients with large perfusion defects (*1–4*). Gating of both rest and poststress perfusion SPECT data is feasible, and a high correlation has been reported between the severity of reversible perfusion defects (i.e., ischemia) and a drop in poststress LVEF (i.e., myocardial stunning) (*5–8*). However, it remains unclear whether this stress-induced drop in EF is related only to myocardial stunning or may be influenced by variations in myocardial perfusion between poststress and rest gated SPECT in patients with coronary artery disease or myocardial ischemia.

When using a same-day protocol, different amounts of radioactivity injected at rest and at stress could potentially influence the evaluation of LV function. In the past, comparison of a rest–stress with a stress–rest 1-d technique showed that the rest–stress protocol had advantages in demonstrating ischemia in segments that were interpreted as being fixed on the stress–rest protocol (*9*). However, only limited data are available about the effect of imaging sequence (rest–stress or stress–rest) on the evaluation of LV function (*10*). When compared with studies in patients, phantom studies have the advantage of allowing control of parameters that may influence either image quality (count statistics or imaging sequence) or the occurrence of myocardial stunning, including the amount and severity of ischemia.

The aim of this study was to assess the respective effects of perfusion defect and image acquisition sequence on evaluation of global LV function using perfusion gated SPECT in a phantom with different degrees of

disease, as a step to developing a large simulated patient database.

MATERIALS AND METHODS

The Dynamic Mathematic Cardiac Torso Phantom

All simulated data for this study were generated using the dynamic 3-dimensional (3D) mathematic cardiac torso phantom (dMCAT 2.01) developed at the University of North Carolina at Chapel Hill (*11*). All generated hearts had the same LVEF (62%), end-systolic volume (ESV; 48 mL), and end-diastolic volume (EDV; 125 mL). This phantom consists of geometric approximations of various organs inside the human upper torso, which can be used to compute radionuclide uptake distribution. According to previous results, 16 frames per cycle were used to represent the heart motion during a single cardiac cycle to minimize temporal undersampling bias (*12*). The distribution of ^{99m}Tc-labeled sestamibi was chosen for modeling the phantom. Compared with the heart, the relative radioactive intensities in soft tissue, blood, lung, liver, kidney, and spleen were 0.03, 0.03, 0.053, 1, 1, and 0.8, respectively. The source distribution was sampled at 64 × 64 pixels with a pixel size of 6.25 mm/pixel. Heart rotation and apical thinning were included in the phantom simulation, but respiratory motion was not included.

Perfusion defects were created separately as localized regions of myocardial uptake. These were scaled relative to the normal wall concentration and then subtracted from the normal heart to yield regions of reduced uptake. Two anterior defects were created: 1 "small" defect approximating half the anterior myocardial wall, and 1 "large" defect calculated as twice the latter defect and approximating the anterior myocardial wall supplied by the left anterior descending artery. As previously described, each defect was scaled to 50%, 75%, and 95% of the activity concentration of the heart and then subtracted from the normal heart (*13*). No segmental wall motion abnormalities were created, so that LVEF remained unchanged in all simulated datasets, regardless of the defect added. Thus, 7 phantoms were created: 1 normal, 3 with a small perfusion defect, and 3 with a large perfusion defect.

Simulation of Gated SPECT Imaging

Projections were generated using a 3D ray-driven projector. Further image manipulations were performed using ImageJ 1.29w software (ImageJ; National Institutes of Health). To simulate collimator blurring, a gaussian stationary 2D blur was added after generating projections. For each dataset, 2 additional acquisitions were simulated by thresholding the projected data to 25% and 75% of the maximum, leading to 21 sets of simulated gated SPECT projection data. Then, a uniform gaussian noise was added (SD = 10) to each dataset. Finally, gated SPECT projection datasets were grouped 2 by 2 to simulate patient data. The effect of scatter was not simulated.

Two series of simulated patients were generated corresponding to 2 different imaging sequences: stress–rest and rest–stress. For each sequence, the first dataset was the 25% thresholded gated SPECT. Both 75% thresholded and 100% signal intensity (SI) were used as a second dataset, corresponding respectively to a 3- and 4-fold increase over the amount of radiotracer usually injected in the clinical setting (*14*). The rearrangement of datasets with different defect sizes and intensities led to the generation of a wide range of simulated myocardial infarction and ischemia. These simulated patients corresponded to normal scans (n = 4), myocardial infarction without ischemia (n = 24), myocardial ischemia without infarction (n = 24), and myocardial infarction with residual ischemia (n = 48).

As a result, 100 simulated datasets were created, corresponding to 50 simulated patients examined twice using both stress–rest and rest–stress sequences. Simulated datasets differed in the amount of myocardial scar or ischemia, but all had the same EDV (125 mL), ESV (48 mL), and EF (62%), with no segmental wall motion abnormalities.

Image Reconstruction and Processing

All projection data were reconstructed and reoriented into 3 orthogonal views with an automated algorithm (MyoSPECT, Vision 5.0.2; GEMS) using filtered backprojection with a Butterworth filter (order, 5.0; cutoff frequency, 0.30 cycles/pixel). For each reconstruction, LV volumes were calculated using automated processing with QGS software (Cedars Sinai Medical Center) (*15*). Perfusion was evaluated on summed nongated images using QPS. This software analysis starts with LV segmentation and the extraction of the 3D endocardial and epicardial surfaces as described for gated and nongated SPECT (*16*). Perfusion at each myocardial sampling point is calculated as the average uptake along a count activity profile (from endocardium to epicardium) normal to the myocardium and passing through that point. In areas of apparent absence of perfusion, endocardial and epicardial surfaces are derived using rule-based criteria ensuring the continuity of surface myocardial count profile. As previously validated, relative segmental myocardial uptake is evaluated using a 20-segment model of the LV and automatically rated using a 5-point scale (from 0 = normal uptake to 4 = no uptake) analogous to that usually used for visual scoring (*16,17*). Summed stress score (SSS), summed rest score (SRS), and summed difference score (SDS) were automatically calculated for each simulated patient with reference to a normal male ^{99m}Tc-sestamibi SPECT database.

Statistical Analysis

Data were expressed as mean value ± 1 SD. Differences between volumes and EFs were calculated using an appropriate paired or unpaired t test. The impact of qualitative parameters on continuous data was evaluated by multiple ANOVA. The interaction between qualitative parameters was tested by the χ^2 test. A P value ≤ 0.05 was considered statistically significant.

RESULTS

The mean values of EDV, ESV, and EF within the 21 originally simulated gated SPECT datasets (before rearrangement) are shown in Table 1. The accuracy of EDV, ESV, and EF measurements was high, ranging respectively from 86% to 95%, 84% to 97%, and 94% to 103% of the true phantom parameters values.

As shown in Table 2, image SI did not significantly influence the measurement of EDV and ESV. However, LVEF was significantly reduced in 25% SI data compared with 100% SI data (60% ± 3% and 63% ± 1%, respectively; P = 0.01).

Impact of Image Sequence

Mean stress EDV was decreased when compared with rest–simulated data (111 ± 4.7 and 112.4 ± 4.8 mL, re-

TABLE 1
End-Diastolic and End-Systolic Values and Ejection Fractions for Defect Severities in Simulated Phantoms

Defect	EDV* (mL)	ESV* (mL)	EF* (%)
No defect	112 ± 5 (90 ± 4)	40 ± 3 (84 ± 7)	64 ± 1 (103 ± 2)
Small defect			
50% max	112 ± 4 (89 ± 3)	42 ± 1 (87 ± 1)	63 ± 2 (102 ± 3)
75% max	119 ± 1 (95 ± 1)	46 ± 5 (97 ± 11)	61 ± 4 (98 ± 6)
95% max	114 ± 3 (91 ± 2)	45 ± 6 (94 ± 13)	61 ± 4 (98 ± 7)
Large defect			
50% max	111 ± 4 (89 ± 3)	41 ± 1 (86 ± 1)	63 ± 2 (101 ± 2)
75% max	107 ± 4 (86 ± 3)	40 ± 2 (84 ± 3)	63 ± 1 (101 ± 1)
95% max	110 ± 2 (88 ± 2)	46 ± 3 (96 ± 6)	58 ± 3 (94 ± 4)

*Values in parentheses represent percentages of true values. True values of parameters in MCAT simulation were EDV = 125 mL, ESV = 48 mL, and EF = 62%.

spectively; $P \leq 0.05$), and mean stress ESV was increased when compared with rest–simulated data (44 ± 4.2 and 42.7 ± 4 mL, respectively; $P < 0.02$). The resulting mean stress EF was decreased in the same comparison (60.3% ± 3.1% and 62% ± 2.7%, respectively; $P = 0.0001$).

As illustrated in Figure 1, calculated stress EDV was decreased, stress ESV was increased, and stress EF was decreased on simulated stress–rest sequences compared with rest–stress data. In contrast, rest EDV was increased, rest ESV was decreased, and rest EF was increased on simulated stress–rest sequences compared with rest–stress sequences. Consequently, the difference (ΔEF) between stress and rest EF (stress EF − rest EF) was more significant when using the stress–rest sequence (−4.8% ± 3%) than the rest–stress sequence (1.3% ± 3.2%; $P < 0.0001$).

Mean SSS and SRS were similar in the stress–rest sequence (23.4 ± 5.6 and 12.8 ± 9, respectively) and the rest–stress sequence (21.9 ± 7.7, not significant; and 15.7 ± 8.9, not significant, respectively), but SDS was higher when calculated on the stress–rest sequence than with the rest–stress sequence (10.6 ± 8.4 and 6.2 ± 8.5, respectively; $P = 0.01$).

Impact of Perfusion Defect

In the generated phantoms, the mean SSS, SRS, and SDS were 22.7 ± 6.7 (range, 0–30; median, 26), 14.3 ± 9 (range, 0–30; median, 14.5), and 8.4 ± 8.7 (range, −9 to 27; median, 7.5), respectively. Summed perfusion scores were categorized according to their median values (SSS = 26; SRS = 14.5). In phantoms with large stress perfusion defects (SSS ≥ 26), stress EDV was lower (109.5 ± 4.1 mL), stress ESV was higher (44.8 ± 4.4 mL), and stress EF was decreased (59.1% ± 3%) compared with the same parameters in phantoms with smaller stress perfusion defects (113.1 ± 4.7 mL, $P < 0.0001$; 43.1 ± 3.9 mL, $P < 0.05$; and 62% ± 2.4%, $P < 0.0001$, respectively). Similarly, in phantoms with large rest perfusion defects (SRS ≥ 14.5), rest EDV (113.3 ± 5.5 mL) was not statistically different, rest ESV (44.6 ± 4.7 mL) was increased, and rest EF (60.8% ± 3%) was decreased compared with the same parameters in a phantom with smaller rest perfusion defects (111.6 ± 3.9 mL, not significant; 40.8 ± 2.1 mL, $P < 0.0001$; and 63.4% ± 1.3%, $P < 0.0001$, respectively).

In phantoms with simulated myocardial infarction (i.e., with a rest perfusion defect, whatever the size) rest EDV was not different from those without myocardial infarction (112.5 ± 5.1 mL and 112.1 ± 4 mL, respectively). In contrast, rest ESV was increased in phantoms with simulated myocardial infarction compared with those without (42.7 ± 4.1 mL and 40.1 ± 2.5 mL; $P < 0.0001$), and consequently, EF was significantly decreased (61.3 ± 2.8 vs. 64 ± 0.8; $P < 0.0001$).

Finally, ΔEF was significant in phantoms with ischemia compared with the same value in phantoms without ischemia (−2.4% ± 4.2% and 0% ± 4.2%; $P < 0.02$). Moreover, linear regression demonstrated a significant correlation between ΔEF and the amount of ischemia evaluated by SDS (Fig. 2). Figure 3 is an example of a simulated stress–rest sequence, with significant ischemia and without infarction, showing a 9% drop in poststress EF.

TABLE 2
Effect of Signal Intensities on Assessment of Left Ventricular Volumes and Ejection Fraction

SI	EDV (mL)	ESV (mL)	EF (%)
25%	110 ± 6	45 ± 6	60 ± 3*
75%	111 ± 4	43 ± 3	62 ± 3
100%	114 ± 3	42 ± 1	63 ± 1

*$P = 0.01$ vs. 100% SI.

Multivariate Analysis

The results of multivariate analysis are summarized in Table 3. The presence of myocardial infarction significantly

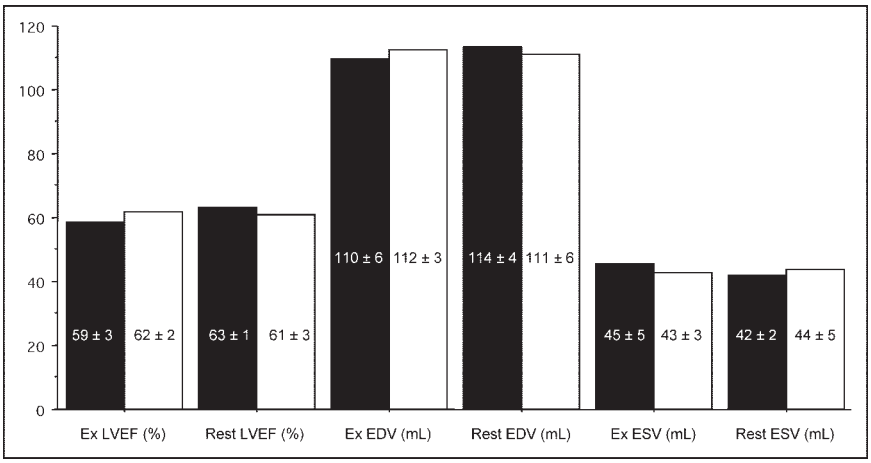

FIGURE 1. Values of LVEF, EDV, and ESV for stress (Ex)- and rest (Rest)-simulated acquisitions for each imaging sequence (stress–rest [black] and rest–stress [white]).

influenced the results of measured rest EDV, rest EF, ΔESV, and ΔEF. The presence of large ischemia (SSS = 26) significantly influenced the results of measured stress EDV, stress EF, and ΔEF. Finally, the simulated acquisition sequence significantly influenced the results of measured stress ESV, stress EF, rest EDV, rest EF, ΔEDV, ΔESV, and ΔEF. The most important factor that influenced the difference between stress and rest EF was the acquisition sequence (F value = 58; $P < 0.0001$). Considering the variation of EF between stress and rest conditions, there was a significant interaction between the presence of myocardial infarction and the choice of acquisition sequence (F value = 14.5, $P < 0.002$). As illustrated in Figure 4, in phantoms with myocardial infarction, stress worsening of EF was observed only with the simulated stress–rest sequence.

Finally, myocardial stunning was defined as a 5% decrease in EF on stress compared with rest SPECT. Although no stunning was present (EF = 62% in all simulations), 24 phantoms (24%) showed myocardial stunning. As shown in Table 4, 23 of those 24 cases (96%) were observed with the stress–rest imaging sequence, resulting in a high association between the stress–rest sequence and the occurrence of myocardial stunning ($\chi^2 = 26$; $P < 0.0001$).

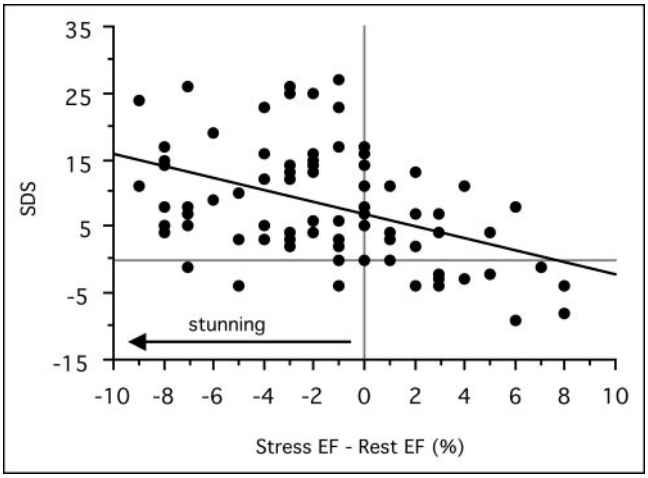

FIGURE 2. Correlation between ΔEF and amount of ischemia evaluated by SDS. $y = 6.815 - 0.911 \times x$; $r = 0.46$; $P < 0.0001$.

DISCUSSION

This study examined the impact of perfusion pattern and imaging sequence on the accuracy of gated perfusion SPECT in determining LV volumes and EF. Absolute results were considered accurate for the evaluation of LV function, but there was a significant influence of low SI on the measurement of EF. When combining data from different SIs to simulate patient acquisitions, we found that both myocardial perfusion and imaging sequence had a significant influence on LV function assessment. Large perfusion defects resulted in an EF decrease as measured by quantitative gated SPECT. Similarly, the use of a stress–rest sequence and not a rest–stress sequence resulted in a reduced stress EF. Consequently, a myocardial stunning artifact was frequently observed when using the stress–rest acquisition sequence.

The accuracy of quantitative gated SPECT has been widely investigated and validated (*2,15,18–20*). In this study, we used a computer simulation with systolic and diastolic volume parameters within published normal ranges (*21–23*). As previously described, SI influenced the measurement of EF, with lower EF observed on the 25% than the 100% SI acquisition. Using a similar mathematic cardiac torso phantom simulation and the same quantitative gated SPECT software, Achtert et al. (*13*) found a comparable 3% underestimation of EF at the lower count levels.

The effect of perfusion defect on assessment of LV function has been suggested but not yet clearly demonstrated (*2,4*). Several studies have shown an underestimation of LVEF measured by means of gated SPECT compared with planar radionuclide angiography in patients with perfusion defects (*2,20*). However, those perfusion defects

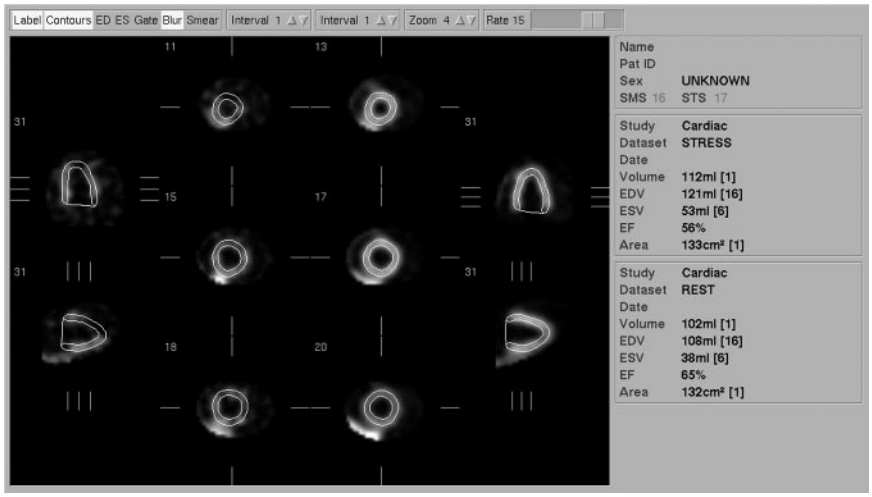

FIGURE 3. Simulated stress–rest sequence showing myocardial ischemia (SSS = 26; SRS = 2; SDS = 24) and a 9% EF decrease on poststress images (stress EF = 56%; rest EF = 65%).

were observed in patients with large myocardial infarction and LV dysfunction. To our knowledge, the effect of large isolated perfusion defects without ischemic LV dysfunction has not been reported. In the present study, perfusion defect significantly influenced the assessment of LV function by affecting EDV or ESV measurement as well as the resulting EF. Poststress EDV and ESV increased and EF decreased in simulated phantoms with large stress perfusion defects. At rest, EF decrease was related to ESV increase without significant EDV increase. Moreover, multivariate analysis confirmed the independent impact of rest and stress perfusion defect on the evaluation of LVEF. This interaction between myocardial perfusion and EF had a major effect on the occurrence of pseudo myocardial stunning, as demonstrated by a 2.4% fall in poststress EF in phantoms with myocardial ischemia. Myocardial stunning (or postischemic dysfunction) is a mechanical dysfunction induced by a brief episode of severe ischemia, which, despite the absence of irreversible cellular damage, persists after the recovery of normal coronary blood flow (*24*). The total recovery of contractile function may require minutes to weeks, depending on the intensity and duration of the ischemic episode. This phenomenon has been demonstrated in clinical settings of transient ischemia and reperfusion, including myocardial infarction, unstable angina, and coronary artery bypass grafting (*25*). Several echocardiographic studies have demonstrated that stunning may occur after treadmill exercise (*26,27*). Poststress myocardial stunning also has been observed in patients with coronary artery disease when examined with gated perfusion SPECT, using both ^{201}Tl- and technetium-labeled tracers (*5,6,8,28–30*). However, in those gated SPECT studies, it remains unclear whether a decreased poststress EF reflected only myocardial stunning or a combination of stunning and perfusion-related artifacts. Heiba et al. (*6*) found a >5% decrease in EF after stress in 20 (45%) of 44 patients with myocardial ischemia. Using ^{99m}Tc-sestamibi gated SPECT, Johnson et al. (*8*) found similar results in 22 (36%) of 61 patients with reversible perfusion defects, although gated SPECT acquisitions were performed 30 min after the completion of exercise. In a

TABLE 3
Multivariate Analysis

Parameter	MI		SSS ≥ 26		Acquisition protocol	
	F	*P*	F	*P*	F	*P*
Stress						
EDV	0.01	NS	9.2	0.0031	3.3	NS
ESV	0.5	NS	1.9	NS	8.1	0.0054
EF	0.9	NS	17.6	<0.0001	30	<0.0001
Rest						
EDV	0.3	NS	0.9	NS	4.2	0.044
ESV	18.8	<0.0001	0.1	NS	1	NS
EF	34	<0.0001	0.3	NS	19	<0.0001
Delta (stress − rest)						
EDV	0.1	NS	2.3	NS	9.1	0.003
ESV	6	0.0159	1.8	NS	8.8	0.0038
EF	9.5	0.0027	10.5	0.0017	58	<0.0001

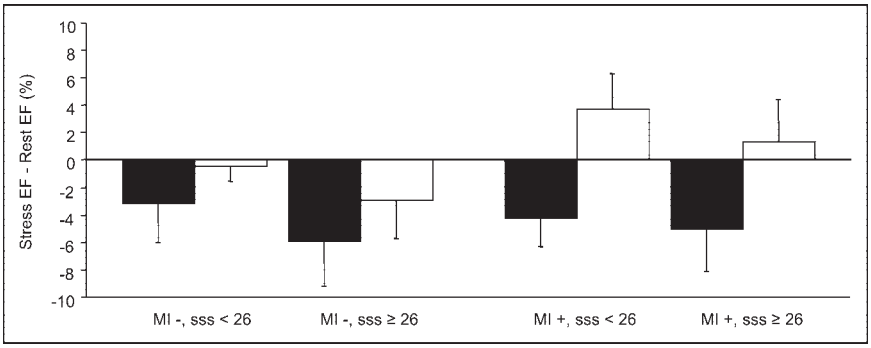

FIGURE 4. Variation of EF between stress and rest (ΔEF) acquisitions (stress–rest [black] and rest–stress [white]). MI = myocardial infarction.

similar population evaluated using exercise and recovery radionuclide angiography, Ambrosio et al. (*31*) emphasized that global EF decreased during exercise in the presence of severe coronary artery disease and ischemia. In the latter study, EF returned to baseline within 10 min, although regional LV function in the ischemic area remained substantially impaired 60 min into recovery. However, delayed recovery of a stress-induced global LV dysfunction can be observed in patients with major myocardial ischemia and regional dysfunction during stress, as a result of severe coronary artery disease (*32*).

In our study, the most important factor influencing the difference between stress and rest EF was the acquisition sequence. When simulating a stress–rest imaging sequence, the underestimation of EF as a result of low SI after stress was incremental with the underestimation related to perfusion abnormalities. As the signal increased on the second simulated acquisition (i.e., rest) and perfusion improved in the ischemic pattern, the conditions for underestimating EF were no longer present at rest. The consequence of these transient conditions was the appearance of a "pseudo stunning" (defined as a 5% decrease in EF) in 23 of 50 (46%) simulated stress–rest acquisitions, although all original simulated phantoms had the same EF. On the other hand, this phenomenon was observed in only 1 rest–stress acquisition where the lower SI acquisitions were used at rest and did not interfere with the largest perfusion abnormalities observed at stress.

In a recent gated SPECT study, Hashimoto et al. (*7*) assessed cardiac function immediately and 20 min after a single peak exercise injection of ^{99m}Tc-sestamibi. In patients with no coronary artery stenosis or scintigraphic evidence of ischemia, there was an overshot of EF immediately after exercise that returned to normal 20 min later. In patients with mild-to-moderate ischemia, EF remained unchanged immediately after exercise and at 20 min thereafter. Finally, in 11 of 47 (23%) patients with severe myocardial ischemia, baseline EF was 53.6% ± 8% and significantly decreased on postexercise scans (45.6% ± 12.1%; $P < 0.01$). Twenty min after exercise, EF further increased to 49.7% ± 10.7% without reaching the baseline level. In this subgroup, the authors used a rest–stress protocol, and in the absence of significant redistribution of ^{99m}Tc-labeled tracers, myocardial perfusion uptake did not differ at 5 and 20 min after stress acquisition. The mean poststress EF decrease was 8%, which is much more significant than the 5% cutoff usually used for assessing myocardial stunning in gated SPECT studies.

TABLE 4
Association Between Imaging Sequence and Observation of Myocardial Stunning*

Imaging sequence	Stunning	No stunning
Stress–rest	23	27
Rest–stress	1	49

*Defined as 5% decrease in stress EF.

Borges-Neto et al. (*10*) evaluated the difference between poststress and rest EF by using a same-day perfusion-function protocol in 126 patients. Patients with and without ischemia had significant differences in poststress versus rest EF (−4.0% and 1.0%, respectively; $P < 0.01$). In a subgroup analysis of those with and without ischemia, the authors concluded that stress–rest (−2.5% and 1.0%, respectively; $P = < 0.05$) and rest–stress (−4.0% and 1.0%; $P = 0.006$) protocols yielded similar results. Nevertheless, this latter study has several limitations. First, patients undergoing exercise (74%) and pharmacologic stress test were pooled. Second, 39 patients underwent a stress–rest protocol whereas many more patients (87) underwent a rest–stress protocol. Third, poststress images were obtained 30 min after the stress injection, a delay that probably underestimated the magnitude of EF changes (*7*). Finally, the absence of statistical analysis of the impact of imaging sequence on the difference between poststress and resting EF did not allow a final conclusion from this series.

Our study had some limitations. All defects were placed in the anterior wall. However, the reliability of quantitative programs may be more affected by an inferior defect, par-

ticularly in the presence of high liver activity. Based on a similar dynamic mathematic cardiac torso phantom simulation, Achtert et al. (*13*) demonstrated that with an increased hepatic uptake of 2 or more times the normal heart uptake, no meaningful EF could be obtained. Consequently, the introduction of a hot liver spot or a severe inferior defect could potentially affect the intrinsic capabilities of the QGS program itself. In this case, it would be impossible to statistically characterize the impact of perfusion defect size, because of the strong interaction between the defect location and QGS properties. For similar statistical considerations we decided to use image sets that were identical with regard to LV chamber sizes, and our results may not be extrapolated to either small or dilated hearts. The investigation of the impact of LV chamber size, as well as transient dilation, would require a specific study design.

The QGS program is a geometry-based algorithm and may be affected by count density, background changes, filtering, and heart size. Using a computer simulation and a patient database, Nakajima et al. (*33*) recently found high correlations between QGS and 3 available programs (4D-MSPECT [University of Michigan], ECT [Emory University], and pFAST [Sapporo Medical University School of Medicine]) for rest EDV and EF assessment, but they did not evaluate the impact of transient LV dysfunction or imaging sequence. In the current study, our goal was to investigate the impact of these latter factors but not to compare geometry versus count-based methods for EF measurement. It remains questionable whether similar results would be obtained with other available programs that are potentially less dependent on geometry for estimation of left ventricular boundaries.

CONCLUSION

Both imaging sequence and perfusion abnormalities influenced the measurement of LV volumes and EF with gated myocardial perfusion SPECT. To avoid these effects in assessing stress-induced LV dysfunction, the rest–stress protocol may be preferable to the stress–rest protocol. Moreover, when using the stress–rest imaging sequence, a poststress EF decrease potentially reflects changes in myocardial perfusion as well as true myocardial stunning.

ACKNOWLEDGMENTS

The authors would like to thank Karen J. Lacroix and Benjamin M. Tsui for use of the dMCAT phantom developed at the University of North Carolina at Chapel Hill, and Richard Medeiros for his advice in editing the manuscript.

REFERENCES

1. Chua T, Yin LC, Thiang TH, Choo TB, Ping DZ, Leng LY. Accuracy of the automated assessment of left ventricular function with gated perfusion SPECT in the presence of perfusion defects and left ventricular dysfunction: correlation with equilibrium radionuclide ventriculography and echocardiography. *J Nucl Cardiol.* 2000;7:301–311.
2. Manrique A, Faraggi M, Vera P, et al. ^{201}Tl and ^{99m}Tc-MIBI gated SPECT in patients with large perfusion defects and left ventricular dysfunction: comparison with equilibrium radionuclide angiography. *J Nucl Med.* 1999;40:805–809.
3. Vera P, Manrique A, Pontvianne V, Hitzel A, Koning R, Cribier A. Tl-gated SPECT in patients with major myocardial infarction: effect of filtering and zooming in comparison with equilibrium radionuclide imaging and left ventriculography. *J Nucl Med.* 1999;40:513–521.
4. Anagnostopoulos C, Gunning MG, Pennell DJ, Laney R, Proukakis H, Underwood SR. Regional myocardial motion and thickening assessed at rest by ECG-gated ^{99m}Tc-MIBI emission tomography and by magnetic resonance imaging. *Eur J Nucl Med.* 1996;23:909–916.
5. Santiago FY, Heiba SI, Jana S, Mirzaitehrane M, Dede F, Abdel-Dayem HM. Transient ischemic stunning of the myocardium in stress thallium-201 gated SPET myocardial perfusion imaging: segmental analysis of myocardial perfusion, wall motion and wall thickening changes. *Eur J Nucl Med Mol Imaging.* 2002;29:979–983.
6. Heiba SI, Santiago J, Mirzaitehrane M, Jana S, Dede F, Abdel-Dayem HM. Transient postischemic stunning evaluation by stress gated Tl-201 SPECT myocardial imaging: effect on systolic left ventricular function. *J Nucl Cardiol.* 2002;9:482–490.
7. Hashimoto J, Kubo A, Iwasaki R, et al. Gated single-photon emission tomography imaging protocol to evaluate myocardial stunning after exercise. *Eur J Nucl Med.* 1999;26:1541–1546.
8. Johnson LL, Verdesca SA, Aude WY, et al. Postischemic stunning can affect left ventricular ejection fraction and regional wall motion on post-stress gated sestamibi tomograms. *J Am Coll Cardiol.* 1997;30:1641–1648.
9. Taillefer R, Gagnon A, Laflamme L, Gregoire J, Leveille J, Phaneuf DC. Same day injections of Tc-99m methoxy isobutyl isonitrile (hexamibi) for myocardial tomographic imaging: comparison between rest-stress and stress-rest injection sequences. *Eur J Nucl Med.* 1989;15:113–117.
10. Borges-Neto S, Javaid A, Shaw LK, et al. Poststress measurements of left ventricular function with gated perfusion SPECT: comparison with resting measurements by using a same-day perfusion-function protocol. *Radiology.* 2000; 215:529–533.
11. Pretorius PH, King MA, Tsui BM, LaCroix KJ, WeishiX. A mathematical model of motion of the heart for use in generating source and attenuation maps for simulating emission imaging. *Med Phys.* 1999;11:2323–2332.
12. Manrique A, Koning R, Cribier A, Vera P. Effect of temporal sampling on evaluation of left ventricular ejection fraction by means of thallium-201 gated SPET: comparison of 16- and 8-interval gating, with reference to equilibrium radionuclide angiography. *Eur J Nucl Med.* 2000;27:694–699.
13. Achtert AD, King MA, Dahlberg ST, Pretorius PH, LaCroix KJ, Tsui BM. An investigation of the estimation of ejection fractions and cardiac volumes by a quantitative gated SPECT software package in simulated gated SPECT images. *J Nucl Cardiol.* 1998;5:144–152.
14. American Society of Nuclear Cardiology. Updated imaging guidelines for nuclear cardiology procedures, part 1. *J Nucl Cardiol.* 2001;8:G5–G58.
15. Germano G, Kiat H, Kavanagh P, et al. Automatic quantification of ejection fraction from gated myocardial perfusion SPECT. *J Nucl Med.* 1995;36:2138–2147.
16. Sharir T, Germano G, Waechter PB, et al. A new algorithm for the quantitation of myocardial perfusion SPECT. II: validation and diagnostic yield. *J Nucl Med.* 2000;41:720–727.
17. Hachamovitch R, Berman DS, Shaw LJ, et al. Incremental prognostic value of myocardial perfusion single photon emission computed tomography for the prediction of cardiac death: differential stratification for risk of cardiac death and myocardial infarction. *Circulation.* 1998;97:535–543.
18. Nakajima K, Taki J, Higuchi T, et al. Gated SPET quantification of small hearts: mathematical simulation and clinical application. *Eur J Nucl Med.* 2000;27: 1372–1379.
19. Vallejo E, Dione DP, Bruni WL, et al. Reproducibility and accuracy of gated SPECT for determination of left ventricular volumes and ejection fraction: experimental validation using MRI. *J Nucl Med.* 2000;41:874–882.
20. Vera P, Koning R, Cribier A, Manrique A. Comparison of two three-dimensional gated SPECT methods with thallium in patients with large myocardial infarction. *J Nucl Cardiol.* 2000;7:312–319.
21. Sharir T, Germano G, Kavanagh PB, et al. Incremental prognostic value of post-stress left ventricular ejection fraction and volume by gated myocardial perfusion single photon emission computed tomography. *Circulation.* 1999;100: 1035–1042.
22. Ababneh AA, Sciacca RR, Kim B, Bergmann SR. Normal limits for left ventricular ejection fraction and volumes estimated with gated myocardial perfusion

imaging in patients with normal exercise test results: influence of tracer, gender, and acquisition camera. *J Nucl Cardiol.* 2000;7:661–668.
23. De Bondt P, Van de Wiele C, De Sutter J, De Winter F, De Backer G, Dierckx RA. Age- and gender-specific differences in left ventricular cardiac function and volumes determined by gated SPET. *Eur J Nucl Med.* 2001;28:620–624.
24. Braunwald E, Kloner RA. The stunned myocardium: prolonged, postischemic ventricular dysfunction. *Circulation.* 1982;66:1146–1149.
25. Bolli R. Myocardial 'stunning' in man. *Circulation.* 1992;86:1671–1691.
26. Kloner RA, Allen J, Cox TA, Zheng Y, Ruiz CE. Stunned left ventricular myocardium after exercise treadmill testing in coronary artery disease. *Am J Cardiol.* 1991;68:329–334.
27. Robertson WS, Feigenbaum H, Armstrong WF, Dillon JC, O'Donnell J, McHenry PW. Exercise echocardiography: a clinically practical addition in the evaluation of coronary artery disease. *J Am Coll Cardiol.* 1983;2:1085–1091.
28. Yamagishi H, Shirai N, Yoshiyama M, et al. Incremental value of left ventricular ejection fraction for detection of multivessel coronary artery disease in exercise ^{201}Tl gated myocardial perfusion imaging. *J Nucl Med.* 2002;43:131–139.
29. Bacher-Stier C, Muller S, Pachinger O, et al. Thallium-201 gated single-photon emission tomography for the assessment of left ventricular ejection fraction and regional wall motion abnormalities in comparison with two-dimensional echocardiography. *Eur J Nucl Med.* 1999;26:1533–1540.
30. Emmett L, Iwanochko RM, Freeman MR, Barolet A, Lee DS, Husain M. Reversible regional wall motion abnormalities on exercise technetium-99m-gated cardiac single photon emission computed tomography predict high-grade angiographic stenoses. *J Am Coll Cardiol.* 2002;39:991–998.
31. Ambrosio G, Betocchi S, Pace L, et al. Prolonged impairment of regional contractile function after resolution of exercise-induced angina. Evidence of myocardial stunning in patients with coronary artery disease. *Circulation.* 1996; 94:2455–2464.
32. Schneider RM, Weintraub WS, Klein LW, Seelaus PA, Agarwal JB, Helfant RH. Rate of left ventricular functional recovery by radionuclide angiography after exercise in coronary artery disease. *Am J Cardiol.* 1986;57:927–932.
33. Nakajima K, Higuchi T, Taki J, Kawano M, Tonami N. Accuracy of ventricular volume and ejection fraction measured by gated myocardial SPECT: comparison of 4 software programs. *J Nucl Med.* 2001;42:1571–1578.